Optical Doping of Silicon

A. Polman
FOM-Institute for Atomic and Molecular Physics
Kruislaan 407, 1098 SJ Amsterdam, The Netherlands
e-mail: polman@amolf.nl

1. Introduction

Silicon is the key element in today's electronic integrated-circuit technology. Unfortunately, Si has an indirect bandgap and therefore shows very inefficient band-to-band optical transitions. As a consequence, Si is considered an impractical material for applications in opto-electronics. An interesting approach to solve this problem is by doping with optically active rare-earth ions. Rare-earths, when incorporated in the trivalent state, have an electronic structure in which the 4f electrons are shielded from the host by closed outer 5s and 5p shells. As a result, relatively sharp, atomic-like intra-4f optical spectra can be observed from rare-earth-doped solids. As an example, Fig. 1 shows a schematic of the energy levels of the erbium 3+ ion. Erbium is of interest because of its transition from the first excited state to the ground state at 1.5 µm, an important telecommunication wavelength. In a semiconductor, a rare-earth dopant may be excited through electrical carriers of which the recombination energy is transferred to the rare-earth ion. Proper defect and impurity engineering is required in order to optimize this energy transfer process. The aim of this extended abstract is to review work on Er doping of Si at the FOM-Institute in Amsterdam, together with the University of Catania. Reference will be given to selected publications in which more detailed information can be found.

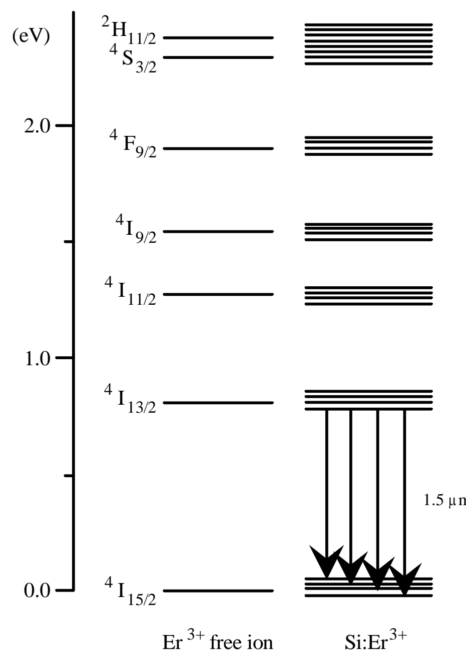

Fig. 1: Schematic energy level diagram of the Er^{3+} ion. When incorporated in a solid, the degenerate levels split due to the Stark effect.

2. Er in Si Goals

In order to obtain efficient photo- or electro-luminescence from Er in Si, several requirements have to be met:

a) high concentrations should be incorporated in single-crystal Si (10^{20} Er/cm^3)

b) the optically active (= luminescent) fraction should be high

c) the minority carrier lifetime should be high, i.e. the Er incorporation procedure should not produce a high density of deep levels in the Si bandgap

d) the Er luminescence efficiency should be long (long luminescence lifetime)

e) the excitation efficiency should be high

If these requirements can be fulfilled, light-emitting diodes with a typical output power of 1 mW may be fabricated. An Er-doped Si laser or optical amplifier with a moderate gain may be feasible as well.

3. Incorporation of Er in Si

The equilibrium solubility of Er in Si is only 10^{14}-10^{16} Er/cm^3. Therefore, high Er concentrations can only be incorporated using non-equilibrium techniques such as ion implantation or molecular beam epitaxy (MBE).

3.1 Ion Implantation

250 keV Er has been implanted into Si(100) at a total fluence of 9×10^{14} Er/cm^2 [1]. The implantation causes full amorphization of a 160 nm thick surface layer of the Si crystal.

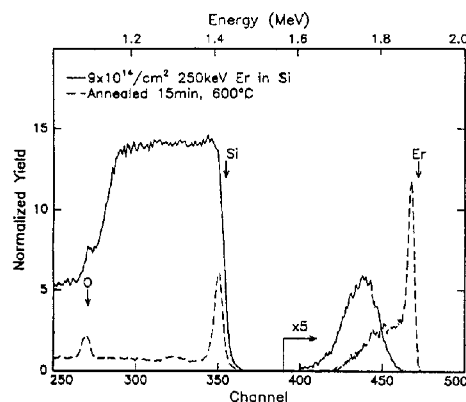

Fig. 2: RBS spectra of Er-implanted crystalline Si (250 keV, 9×10^{14} Er/cm^2), before and after annealing at 600 °C (from ref. [1]).

This is shown in Fig. 2 which shows a 2 MeV Rutherford Backscattering Spectrometry (RBS) spectrum of the implanted sample. The high yield in the channels between 260 and 355 corresponds to the disordered Si layer; the Gaussian profile between channels 400 and 460 corresponds to the Er depth profile in the amorphous layer. After thermal annealing at 600 °C for 15 min the amorphous layer recrystallizes by solid phase epitaxial (SPE) layer-by-layer regrowth. The yield in the Si part of the spectrum decreases, and a nearly perfect crystal is formed. During recrystallization, segregation and trapping

of Er takes place at the moving amorphous-crystal interface. Finally, 65 % of the Er is trapped in the crystal and 35 % ends up at the surface. In this way, up to $1.0x10^{20}$ Er/cm^3 is incorporated in single crystal Si. Details of the temperature and concentration-dependence of the crystallization, segregation and trapping processes, and a model which describes the role of defects in the amorphous layer near the interface, are described in a separate paper [2].

3.2 Molecular Beam Epitaxy

Erbium-doped epitaxial Si layers were grown on Si(100) in an MBE apparatus utilizing an electron-beam evaporator for Si and a Knudsen cell for co-evaporation of Er [3]. The substrate temperature was 600 °C, and the base pressure $3x10^{-11}$ mbar. Fig. 3 shows Er depth profiles derived from RBS spectra taken after growth at two different Er fluxes (indicated in the figure). The Si flux was $1.5x10^{13}$ Si/cm^2s. In all cases, segregation and trapping of Er takes place. This can be seen in Fig. 3(a), which shows the Er profiles after growth of 60 and 100 nm thick layers. The Er surface concentration increases with growth thickness. The trapped Er concentration also increases with thickness. A two-dimensional kinetic segregation and trapping model that explains the data is described in Ref. [3]. When the Er deposition rate is increased (Fig. 3(b)) a sudden breakdown in the growth mode is observed when the Er concentration reaches a critical level ($2x10^{14}$ Er/cm^2 at the surface, $2x10^{19}$ Er/cm^3 in the crystal). At that stage an abrupt increase in the Er concentration is observed. This is attributed to the formation of erbium-silicide precipitates as the Er surface coverage reaches a critical value. Such precipitates can be epitaxially aligned along (111) planes in the Si crystal [3].

The segregation and trapping of Er can be completely avoided when MBE is performed in an O_2 ambient at a pressure of $4x10^{-10}$ mbar. This can be seen in Fig. 4, which shows a comparison of Er depth profiles for 100 nm thick films grown with and without oxygen. The effect of O is though to be due to the formation of Er-O complexes, which are more easily incorporated in the crystal than Er alone. A similar effect of O inhibiting the segregation of Er has also been seen in experiments on recrystallization of Er-doped amorphous Si co-doped with oxygen [2].

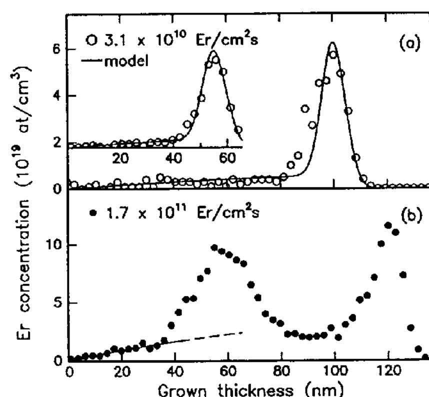

Fig. 3: RBS spectra of Er-doped crystalline Si films grown by MBE, for two different Er deposition rates (indicated in the figure). The Si deposition rate was $1.5x10^{13}$ Si/cm^2s and the substrate temperature 600 °C (from ref. [3]).

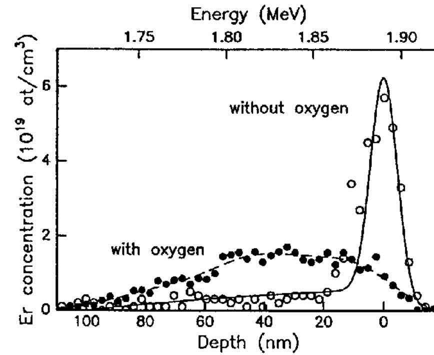

Fig. 4: RBS spectra of Er-doped Si grown by MBE in an O_2 ambient at a pressure of 4×10^{-10} mbar (from ref. [3]).

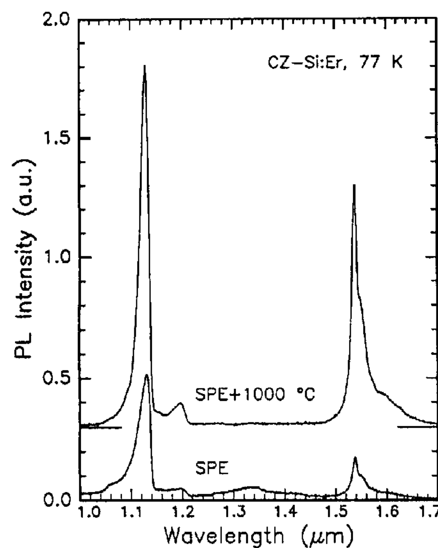

Fig. 5: Photoluminescence spectra taken at 77 K of Er-implanted Si(100) (9×10^{14} Er/cm^2, 250 keV) after solid phase epitaxial crystallization (SPE) at 600 °C, and after a subsequent anneal at 1000 °C for 15 sec. The excitation wavelength was 514 nm (from ref. [4]).

4. Photoluminescence of Er in Si

Fig. 5 shows photoluminescence (PL) spectra of Er-implanted (9×10^{14} Er/cm^2, 250 keV) Si(100) after recrystallization at 600 °C, and after a subsequent anneal at 1000 °C for 15 sec [4]. The spectra are taken at 77 K. Clear Er-related luminescence around 1.54 μm is observed, characteristic for the $^4I_{13/2} \rightarrow {}^4I_{15/2}$ intra-4f transition of Er^{3+} (see Fig. 1). Near band-edge luminescence around 1.13 μm is also seen. Photoluminescence excitation spectroscopy data (not shown) indicate that Er in Si is excited through photogenerated carriers, and not by direct optical absorption [4]. In both cases in Fig. 5 the Er luminescence lifetime is roughly 1 ms. This is thought to be close to the radiative lifetime, and therefore the luminescence efficiency is quite high at 77 K. The increase in Er PL intensity upon annealing at 1000 °C is attributed to an increase in excitation efficiency due to an increase in the minority carrier lifetime upon annealing.

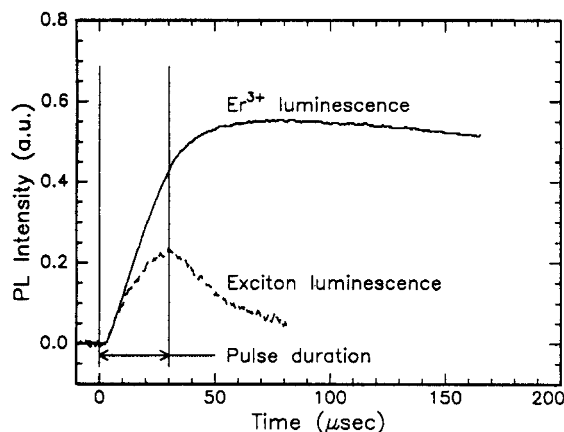

Fig. 6: Time-resolved photoluminescence spectra taken at 9 K for Er-implanted Si ($7x10^{14}$ Er/cm^2, 1.5 MeV, annealed at 600 °C and at 1150 °C). The timing of the 30 µs excitation pulse at 488 nm is shown by the vertical lines. Signals for both the Er luminescence at 1.54 µm and the exciton luminescence at 1.12 µm are shown (from ref. [5]).

To get further insight in the excitation mechanism, time-resolved PL measurements were performed [5]. Fig. 6 shows the time dependence of the Er-related 1.54 µm emission and the near-band edge 1.2 µm emission, after short pulse (30 µs) excitation at 515 nm. The data were taken at 9 K. As can be seen, after the excitation pulse is switched off the Er signal continues to increase, while the band edge signal shows an immediate decay (limited by the time resolution of the detector). The delay in Er excitation is characteristic for an impurity-Auger excitation process (see Fig. 7): a electron-hole pair is first bound at an Er-related defect in the crystal (represented by a defect level in the bandgap). This is a fast process, as the minority carrier lifetime is well below 1 µs. Subsequently, the pair recombines and the energy is transferred to the Er^{3+} ion. A photon at 1.54 µm may then be emitted as the Er returns to the ground state. The delay in Fig. 6 then reflects the characteristic time for the energy transfer from the Si electronic system to the Er interatomic system. Although shorter, the time delay has been observed up to temperatures as high as 100 K, indicating that this energy transfer mechanism is valid also at high temperatures.

One problem in the application of Er in Si is the luminescence quenching which is observed as the temperature is increased. In fact, above 200 K virtually no luminescence is observed from Er-doped Si (either Czochralski or float-zone grown) [6]. Between 77 and 200 K the quenching is due to an increase in the non-radiative decay rate. At higher temperatures it may also be due to a reduction in the excitation efficiency [6]. The temperature quenching can be dramatically reduced by the addition of impurities such as oxygen [6] – [9]. It is believed that Er acts as a microscopic getter for O, and Er-O complexes are formed [4]. Such a complex will have a different position in the bandgap than pure Er (see Fig. 7), which may result in a different temperature dependence of the excitation and/or deexcitation rate, hence different quenching.

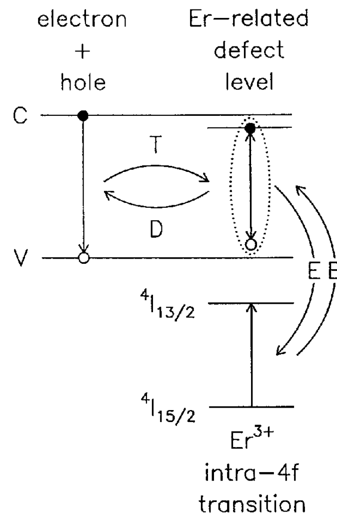

Fig. 7: Schematic of impurity Auger excitation process of Er in Si.

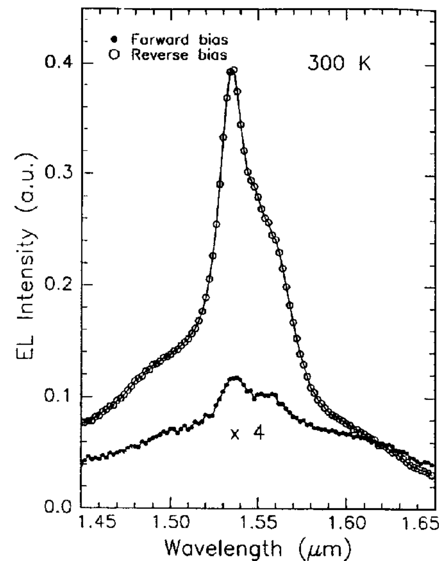

Fig. 8: Room-temperature electroluminescence from an Er-doped crystalline Si p-n diode. Spectra are shown at a fixed current density of 2.5 A/cm^2 under forward and reverse bias (from ref. [10]).

5. Electroluminescence of Er in Si

A p-n diode structure was prepared in crystal Si, and Er and O were implanted in the depletion layer of the device [10]. Fig. 8 shows room-temperature measurements of the luminescence of this device at a current density of 2.5 A/cm^2. Under forward bias (+1.4 V) clear electroluminescence is observed around 1.54 μm, which is attributed to electrically generated carriers which recombine and transfer energy to Er in the depletion region at the junction. A much higher signal is observed under reverse bias (-5.3 V). Under these conditions the device is in the breakdown regime. The

luminescence from Er is attributed to impact excitation of Er by hot carriers which are accelerated through the junction.

The internal quantum efficiency in this device was in the range 10^{-5} – 10^{-4}. More research is required to increase this number, for example by increasing the optically active fraction, further reduction of the luminescence quenching, and by optimization of the device design.

6. Conclusions

Erbium-doped silicon shows room-temperature photo- and electroluminescence at 1.54 µm due to an intra-4f transition of the Er^{3+} ion. The Er can excited through an impurity Auger effect, in which the recombination energy of an electron-hole pair is transferred to the Er ion, or by impact excitation. Non-equilibrium techniques such as ion implantation and molecular beam epitaxy are used to incorporate high concentrations of Er in Si. Proper defect and impurity engineering is required to optimized the luminescence efficiency.

Acknowledgments

This work is part of the research program of FOM and was made possible by financial support from NWO, STW and IOP Electro-optics. Part of this work was performed in collaboration with the University of Catania. This abstract is a review of work in the past few years; reference to the researchers involved is made in the papers referenced in the text.

References

[1] A. Polman, J.S. Custer, E. Snoeks, and G.N. van den Hoven, Appl. Phys. Lett. **62**, 507 (1993).

[2] J.S. Custer, A. Polman, and H.M. van Pinxteren, J. Appl. Phys. **75**, 2809 (1994).

[3] R. Serna, M. Lohmeier, P.M. Zagwijn, E. Vlieg, and A. Polman, Appl. Phys. Lett., in press (March 13, 1995 issue).

[4] A. Polman, G.N. van den Hoven, J.S. Custer, J.H. Shin, and R. Serna, J. Appl. Phys. 77, 1256 (1995).

[5] Jung. H. Shin, G.N. van den Hoven, and A. Polman, submitted to Appl. Phys. Lett.

[6] S. Coffa, G. Franzò, F. Priolo, A. Polman, and R. Serna, Phys. Rev. B **49**, 16313 (1994).

[7] R. Serna, E. Snoeks, G.N. van den Hoven, and A. Polman, J. Appl. Phys. **75**, 2644 (1994).

[8] S. Lombardo, S.U. Campisano, G.N. van den Hoven, A. Cacciato, and A. Polman, Appl. Phys. Lett. **63**, 1942 (1993).

[9] G.N. van den Hoven, A. Polman, S. Lombardo, and S.U. Campisano, submitted to J. Appl. Phys.

[10] G. Franzò, F. Priolo, S. Coffa, A. Polman, and A. Carnera, Appl. Phys. Lett. **64**, 2235 (1994).